

Multifidelity Approaches for the Computational Analysis and Design of Effective Flapping Wing Vehicles

David J. Willis ^{*}; Per-Olof Persson [†]; Emily R. Israeli [‡]; Jaime Peraire [§]

Sharon M. Swartz [¶]; Kenneth S. Breuer ^{||**}

In this paper we review several computational aerodynamics tools which we are using to examine and understand flapping flight. The computational methods incorporate different levels of geometric and physical modeling fidelity, ranging from simplified models which determine optimal wake vorticity distributions (eg. Hall et al.¹⁻³) to accurate descriptions of the flow physics. By exploiting multiple fidelity levels, computations can be efficiently performed at the required fidelity level making design and analysis a more efficient task.

Several computational results are presented illustrating the versatility of the computational methods which are presented. The computational investigations explore top-down and bottom-up philosophies to enhance the understanding of flapping flight physics, force production and energetics. The results which are discussed range from simple two dimensional prescribed motions, to three-dimensional aerodynamics simulations of geometrically accurate bat flight.

I. Introduction

The following paper is a review of a compilation of work which has been previously presented or will appear.^{4-9,52,53} Much of this work derives from computational investigations which use different elements of a multi-fidelity computational framework. The computational framework and results which are shown represent an ongoing effort to understand flapping flight.

Modern aircraft analysis, design and optimization relies on computational tools of differing physical and geometrical fidelity levels. These different computational tools exploit simplifications and assumptions in order to reduce computational complexity where appropriate. Although high accuracy simulations using high fidelity representations of the underlying physics are desired at each level of the design process, computational complexity places severe restrictions, often resulting in the use of lower fidelity and approximate methods in the early design stages. Due to the high Reynolds numbers and the aerodynamic shapes involved in aircraft design, many of those flows can be well approximated using simplified governing equations, such as the Euler equations^{10,11} or the potential flow equation.^{12,14,15} It is due to these simplifications in the governing equations that rapid analysis tools can be used with great success in the early stages of the design process.

With the increased interest in developing Uninhabited Micro Aerial Vehicles (UAVs and MAVs), attention has turned from traditional tube-wing aircraft configurations to less conventional designs. Due to the small scale, and the lack of passenger imposed limitations, these aircraft represent a rich opportunity to explore novel concepts which may benefit from exploiting non-traditional flow physics. Many of the potential designs employ large deformation fluid-structure interactions³⁰⁻³² as well as active and passive wing morphing.^{5,33}

^{*}Research Scientist, Department of Aeronautics and Astronautics, MIT

[†]Instructor, Department of Mathematics and Statistics, MIT

[‡]Graduate Student, Department of Aeronautics and Astronautics, MIT

[§]Professor, Department of Aeronautics and Astronautics, MIT

[¶]Associate Professor, Department of Ecology and Evolutionary Biology and Division of Engineering, Brown University.

^{||}Professor, Division of Engineering, Brown University.

^{**}The authors of this paper would like to thank the SMA, AFOSR and the NSF for their support of different elements of this work.

Of particular interest is the development and application of computational tools which can be used in the design and analysis of the unsteady fluid structure interactions associated with flapping and morphing wing aircraft. For the case of efficient flapping flight, the current aeronautical tool-set is likely to provide good initial insights in the design space.

In this paper we present a collection of computational tools⁵ which have been developed and modified to analyze characteristic problems in flapping flight. The framework consists of a suite of tools including (1) wake only analysis approaches,^{1-5,16} (2) a modern panel method^{17,18} and (3) a high order discontinuous Galerkin Navier-Stokes solver.^{52,53} At present, a ubiquitous structural approach is being pursued which will be able to seamlessly couple to several of the computational aerodynamics/fluid dynamics methods. The framework mirrors several of the analysis tools used in aircraft design, namely (1) Trefftz Plane Analysis (2) Lifting Line/Panel Methods and (3) Navier-Stokes solution methods. As in aircraft analysis and design, lower fidelity, faster computational methods are preferred for preliminary design space exploration and analysis, while the more physically and geometrically accurate models are used for detailed analysis and design fine tuning. Although, we present a computational framework in this paper, it is by no means the only (or optimal) choice of tools for examining the problems under consideration. For example, in the past, several different combinations and manifestations of these methods have been used to examine flapping flight.¹⁹⁻²¹

In order to understand flapping flight, a philosophy involving both top-down and bottom-up analysis is being examined. The *top-down* approach explores existing successful designs (natural flapping flight) for insight and inspiration. The biological inspiration for this work comes from the study of bats in flight.^{6,23,54} Bat flight is being studied with the desire to understand the fluid dynamics, structural dynamics as well as the kinematics of successful flapping. Since bats possess impressive capabilities including higher flight efficiency than other flying animals of a similar size,²⁵⁻²⁷ high maneuverability,²⁸ and precise flight control capabilities, they make a compelling case study. Unfortunately, even if a perfect simulation of bat flight could be performed, it would not be immediately clear which parameters govern flight efficiency and which are dominated by biological or design constraints. In order to gain a deeper understanding of parametric dependencies in flapping flight, a *bottom-up* analysis approach is simultaneously being explored. For this, the effects of the different kinematic, structural and control strategies are being examined and cataloged. One example of this bottom-up philosophy would be to explore the benefits of forward-aft kinematics of flapping on the overall aerodynamics of flight, and determine the efficiency and flight control benefits of such a parameter.

I.A. Efficient Flapping Flight

Two of the dominant limitations of modern MAVs are the storage of sufficient energy to enable long range or long duration MAV missions, and the lack of maneuverability and control (eg. gust sensitivity, inability to perch, hover, etc.). Although the energy constraints can be partially attributed to inefficient power conversion (eg: battery technologies, mechanisms), inefficient flight systems and designs are equally responsible for this lack of capability. In terms of maneuverability and control, the low Reynolds number flight regime in which these vehicles fly imposes significant constraints on traditional control strategies. As a result of both of these constraints, we have turned to flapping flight and nature for inspiration. In nature, both efficiency and maneuverability appear to be fine tuned for this Reynolds number regime. In this overview paper, we explore the concepts surrounding efficient flight, leaving maneuverability to future investigations.

Traditionally, efficient flight vehicle designs are generated by reducing aerodynamic drag. In order to do this, wing designs with minimal separation and low induced (and wave) drag have been explored with great success. In modern aircraft, flight performance has reached a point where only small improvements in efficiency can be made. With regard to flapping flight efficiency, it would appear that nature persists in outperforming any human generated designs. In this work, an approach similar to traditional aircraft design is being pursued for exploring and maximizing flapping flight performance. The effects of wake induced power losses are examined using simple potential flow methods such as the wake only methods of Hall et al¹⁻³ and panel methods.⁵ In addition to minimizing induced losses, viscous losses remain a concern. As such, higher fidelity Navier-Stokes approaches are being used to examine and confirm the predicted effects of viscosity and presence of separation in the flows of interest.

Unfortunately, the pursuit of efficient flight strategies is not as straight forward as it is in traditional aircraft applications. One of the primary concerns in efficient MAV flight is the lack of solid understanding of the transitional flow physics of the Reynolds number regime in which these vehicles operate. MAVs as well as small bats and small birds operate in a flow regime which is associated with unpredictable transitional

flow ($Re = 15,000-70,000$).⁵⁵ These features of the flow regime challenge the applicability of potential flow methods for examining these flows, making high fidelity confirmation of results and designs a necessity. We contend however, that potential flow models augmented with (sometimes simple) viscous corrections can provide decent trend information for light and moderately loaded wings.

II. Computational Model Fidelity Levels

In this section we briefly present several different computational tools which are capable of providing insight into flapping flight aerodynamics performance. Although the problem considered is predominantly multidisciplinary (aerodynamics, structures, bio-chemical, physiological and controls), the aerodynamics of a design are a fundamental component of efficient flight. High aerodynamic efficiency is achieved by presenting appropriate shapes to the flow, which, can be accomplished through the assistance of any of the disciplines aforementioned.

Due to the brief description of the computational methods, the reader is referred to the detailed references associated with each method, or to the work describing the multi-fidelity framework.⁵

II.A. Potential Flow Methods

Potential flow methods represent a powerful approximation of aerodynamic flows when they are applicable. The assumptions which are involved in reducing the governing fluid equations to a potential flow are (1) irrotational flow, (2) inviscid flow, and (3) incompressible flow. The time dependence in unsteady potential flows is captured by the time dependent vortex wake history and the unsteady Bernoulli equation which is used to compute the pressure. As such, steady potential flow methods are relatively easily extended to model unsteady flows by implementing approaches to handle time varying wakes.

Potential flow modeling is routinely used in the aeronautical industry for approximating high Reynolds number flows with limited viscous effects (thin boundary layers with little to no flow separation). Since potential flow methods are typically much simpler to discretize and solve, they present an attractive alternative to high fidelity simulations. In our current research into efficient flapping flight, potential flow methods play an important role in design space exploration and preliminary evaluation of candidate flapping geometries. Although the applicability of these methods may be suspect in some cases, the methods can provide a good approximation of the trends encountered, and solutions often provide indications of possible failures in modeling assumptions.

II.A.1. Wake Only Methods: HallOpt

Wake only methods¹⁻³ for predicting optimal wake vorticity distributions in flapping flight provide powerful approximations of how flight forces are efficiently generated. In their work, Hall et al.¹⁻³ also present simple viscous loss augmentations to the wake only potential flow method for computing the minimum power requirements for flapping flight. The resulting method can provide a first estimate of upper efficiency bounds. In the method, a given periodic wake shape is represented using a vortex-lattice discretization, and the unknown optimal vorticity distribution is determined by minimizing the flight power expression subject to the period-average flight force constraints. This elegant method can be used to rapidly determine optimal wake vorticity distributions for a particular wake shape and a particular desired set of forces.

The wake only method, HallOpt, provides useful insight into the flapping flight parameter space,⁴ and has also been used in preliminary design stages to initiate designs for efficient three dimensional flappers.⁵ The method is extremely attractive in a design setting since it is only dependent on the wake shape and the desired flight forces. It does not require a detailed description of the flapping wing geometry. In fact, by solving for the optimal vorticity distribution in a given wake, the HallOpt method provides insight into the possible wing shapes that can be used to produce the optimal wake vorticity distribution. In addition, since the method does not require detailed geometry information, initial design space sweeps for parameter dependencies are easily, and rapidly performed.

II.A.2. Panel Methods : FastAero

Panel methods provide a trade-off between computational speed and accuracy by exploiting a surface only, boundary element method to solve the potential flow equation. The use of a surface-only discretization

is particularly attractive for the large unsteady motions and deformations encountered in flapping flight. Not only is the solution time drastically reduced due to the lower number of unknowns, but the time and effort required to generate discrete geometry representations is reduced by a full dimension (surface vs. volume meshing). In panel methods the geometry under consideration is represented accurately; however, the flow remains a linear potential flow, and as such does not model viscous effects. Unsteady potential flow aerodynamics effects are accurately modeled using these methods, enabling an estimation of the unsteady effects on the overall flow.

The panel method framework, *FastAero* which is considered in this work is capable of solving both the Neumann and Dirichlet boundary condition formulations using unstructured, linear-basis, discretizations of the doublet-velocity and source-doublet-potential methods respectively. Both two- and three-dimensional versions of the potential flow solvers have been implemented, providing the capability to compare results with lower and higher fidelity solution methods. The source-doublet potential method is described in previous work,^{7,24} and the doublet-velocity method is similar to a doublet lattice method.^{12,35}

In the doublet lattice formulation, the boundary integral equation is discretized and solved using the boundary element method.^{12,14,36} The discretization of the surface doublet strengths is performed using linear basis functions on triangular panels.⁷ The boundary conditions are satisfied using a Galerkin procedure in which the outer integral is evaluated numerically²⁴(the panel to evaluation point integrals are evaluated using analytic expressions^{13,14}). The use of linear panels provides a rapid means for computing the velocity and pressure jumps across the membrane surface (an unsteady Bernoulli equation is used for computing the pressure jump). The Kutta condition which is applied requires that the doublet strength be continuous at the trailing edge, with increases in wing-bound circulation being matched with corresponding increases in wing shed vorticity in the wake (satisfying Kelvin’s Theorem). In addition, a weak iteration nonlinear Kutta condition enforcing pressure equality at the trailing edge can be used. Once uniquely defined, the wake vorticity can be represented using either sheets or vortex particles.^{12,24,37} The use of vortex particles allows a method which advects the vorticity simply with the local velocity,^{7,24} while also permitting a fixed-in-space wake. Finally, in order to render the three-dimensional unsteady potential flow solution efficient on workstations and personal computers, the precorrected-FFT⁴⁰ and Fast Multipole Tree^{41,42} solution acceleration techniques are implemented. At the present time, we are considering extending the panel method framework to permit vorticity shedding from user prescribed separation points¹² (in two dimensions) or lines¹² (in three-dimensions). This added functionality should further enhance the predictive capability of these methods and allow for first order flow estimates in separated flows and permit modeling of larger scale features such as leading edge vortices.

II.B. High Fidelity Methods

The methods described thus far are accurate for flows in which viscous effects and flow separation are minimal. Unfortunately flapping flight presents a design space in which separation can easily occur (due to the large relative motions which are possible). Although viscous corrections and predictions can be applied in potential flow, modeling viscous effects such as large regions of separation or regions of re-circulating flow, requires higher fidelity physics solvers based on the full Navier-Stokes equations. Several options exist for modeling the unsteady, morphing geometry Navier-Stokes equations. Of these methods, several approaches have found success in flapping foil and wing applications. The first approach is the family of immersed boundary methods,^{44,45} and the second approach is the Arbitrary-Lagrangian-Eulerian (ALE) approaches. In the computational framework considered, a high order, discontinuous Galerkin ALE approach is being pursued.

II.B.1. Discontinuous Galerkin Arbitrary-Lagrangian-Eulerian (ALE) Navier-Stokes: 3DG

Our high fidelity simulation tool is a high-order accurate solver based on the discontinuous Galerkin method⁴⁹ and the CDG scheme for viscous terms.⁵⁰ It solves the Navier-Stokes equations efficiently for a wide range of Reynolds numbers and Mach numbers,⁵¹ and it uses an ALE formulation based on mapping which achieves arbitrary high orders of accuracy in space and time.⁵² The computational domain is discretized with unstructured simplex meshes which allows for complex geometries and local adaptation. The code has also been integrated with structural models, for fully coupled fluid-structure interaction simulations.⁵³

III. Examples, Simulations and Investigations

In this paper, several examples using the multi-fidelity computational framework are presented. Several of these examples have been previously published^{4,5} or are in preparation.^{6,46} The different examples are chosen to illustrate the use of multi-fidelity approaches for flapping flight and propulsion.

III.A. Example 1: Prescribed Motion for 2D Airfoils

In this example, a series of simulations of a two-dimensional airfoil (HT-13) undergoing prescribed motions are presented. This series of test cases compares the predictive capability of potential flow methods with Navier-Stokes solvers in aggressive unsteady flows. The example is similar to studies of airfoils undergoing sudden startup motions,⁵⁶ as well as other investigations of pitching and heaving airfoils.^{22,29,47}

III.A.1. Flapping Motions

The parameters of the experiments have been chosen so that they are approximately characteristic of flapping in nature. The characteristic non-dimensional values are approximate for the mid-semi-span wing section (located near the bat's wrist) of a flapping bat wing (see table 1).

| Parameter | Value |
|--|-------|
| Reduced Frequency : $k = \frac{\omega c}{2U_\infty}$ | 0.4 |
| Flapping Amplitude Ratio : $\Delta h/c$ | 1.0 |

Table 1. The dimensionless parameters associated with the unsteady 2-Dimensional flapping experiments. The experiments aim to explore a parameter space similar to bat flight.

When using high fidelity computational methods, the flow is simulated at a Reynolds number of 5,000. This Reynolds number was chosen to enable rapid simulations of the flow avoiding turbulence models or fine boundary layer meshes. Although the Reynolds number is lower than what one might expect to find in bat flight ($Re \simeq 15,000 - 35,000$), the simulations are expected to exhibit the correct trends. Although the experiments which are presented exploit characteristic non-dimensional quantities, the resulting flows are unlikely to be representative of the actual flows found in bat flight or flapping MAV designs. Significant differences will arise due to three-dimensional effects as well as compliant wing structures; however, this simple exploration of a small portion of the flapping design space provides useful insight into the applicability of the lower fidelity computational methods. The following examples are run using both high and medium fidelity flow solvers.

III.A.2. Prescribed Pitch Change : 2D Airfoil

In this exploratory problem, a time dependent change of airfoil pitch, $\theta(t)$ is prescribed according to the following relationship:

$$\theta(t) = \begin{cases} 0 & \text{for } t < t_a \\ -\theta_0 + \theta_0 \cos(\omega t) & \text{for } t_a \leq t \leq t_a + \frac{\pi}{\omega} \\ -2\theta_0 & \text{for } t > t_a + \frac{\pi}{\omega} \end{cases} \quad (1)$$

The use of unsteady prescribed pitch motions is an overly simple model of flapping, but is useful to examine the predictive capability of potential flow methods. The pitch only investigation permits a first observation of unsteady effects and changes in local incidence on the flow. Although the effects of unsteady changes in the local incidence can be explored, the lack of a prescribed heaving motion means the unsteady effects of more characteristic flapping motions are not present. In this example the following parameter values which are considered are listed in table 2. The time history of the force and moment coefficients for the airfoil pitch change are presented in Figure 1. Several characteristic snapshots are shown in Figures 7-8, and some features of interest are observed:

1. The initial flow startup has attached flow for a time interval after the motion has started, even when the incidence of the airfoil is greater than the expected static stall angle. The combined effect of the acceleration of the airfoil and the induced wake velocity likely provides separation delay mechanisms,

| Parameter | Value |
|------------|-------------|
| θ_0 | 0, 3, ...18 |
| ω | 0.8 |

Table 2. The parameter values for the pitch-up case. Notice that the pitch angle will become extreme at large values of the pitch.

much like the case of sudden startup flows;⁵⁶ however, in this example, due to the more gradual startup (as opposed to sudden startup) the formation of separated flow regions such as leading edge separation bubbles takes a longer time (the airfoil travels several chord lengths before leading edge separation effects become noticeable). The potential flow methods accurately predict this initial startup due to their ability to model unsteady attached flows.⁵⁶

2. Following the initial startup phase a region of separated flow appears on the leading edge region of the aggressively pitched airfoils. The presence of this bubble, when it is small, does not significantly change the predictive capability of the potential flow; however, as the separated region grows, deviations between the potential flow and Navier-Stokes models become more pronounced.
3. In cases where the prescribed pitch is very aggressive, the region of separated flow on the suction side of the airfoil separates completely from the airfoil, forming a trail of periodically shed vortices in the wake of the airfoil. This separation is accompanied by a loss in lift and a rapid increase in drag. The force generation at this point is characterized by significant unsteadiness and is not at all accurately modeled using potential flow methods. This operating point is undesirable from both an efficiency and a controllability standpoint, unless large drag forces are required to slow the vehicle down.
4. The lift coefficients which are predicted in both the potential flow and high fidelity Navier-Stokes solver are large (especially for aggressive pitch angles). By exploiting unsteady airfoil motions, high lift coefficients can be generated. These lift coefficients, although accompanied by sharp increases in the drag, initially provide a well defined relationship between pitch angle and lift generation with respect to time.

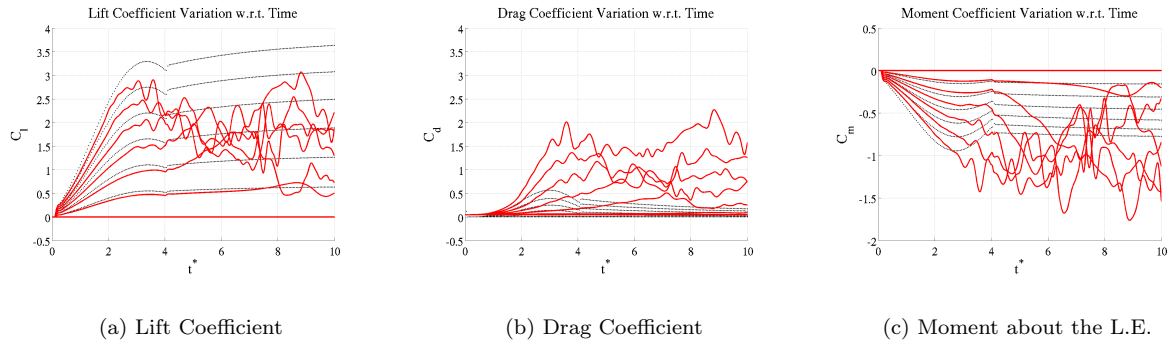


Figure 1. The force and moment coefficient evolution with respect to time for the pitch only case. The pitch motions commence at $t^* \simeq 0.1$ and end at $t^* \simeq 4$. The most aggressive pitch angle change is 36 degrees. In these examples the potential flow results are represented using black ‘,’ while the Navier-Stokes simulation results are illustrated using red lines. The initial characteristics of the lift and moment coefficients appear to be well predicted by both of the models. As might be expected, the drag coefficient has significant deviations due to the lack of a viscous correction in the potential flow model.

III.A.3. Prescribed Pitch and Heave : 2D Airfoil

In this example a simple pitch and heave motion is combined into a single down-stroke-like motion. The motions are described using the following relationships:

$$h(t) = \begin{cases} h_0 & \text{for } t < t_a \\ h_0 \cos(\omega t) & \text{for } t_a \leq t \leq t_a + \frac{\pi}{\omega} \\ -h_0 & \text{for } t > t_a + \frac{\pi}{\omega} \end{cases} \quad (2)$$

$$\theta(t) = \begin{cases} 0 & \text{for } t < t_a \\ \theta_0 \sin(2\omega t) & \text{for } t_a \leq t \leq t_a + \frac{\pi}{\omega} \\ 0 & \text{for } t > t_a + \frac{\pi}{\omega} \end{cases} \quad (3)$$

The above prescribed motions were selected due to the continuity of the first derivatives of the motion. The parameters explored are listed in table 3.

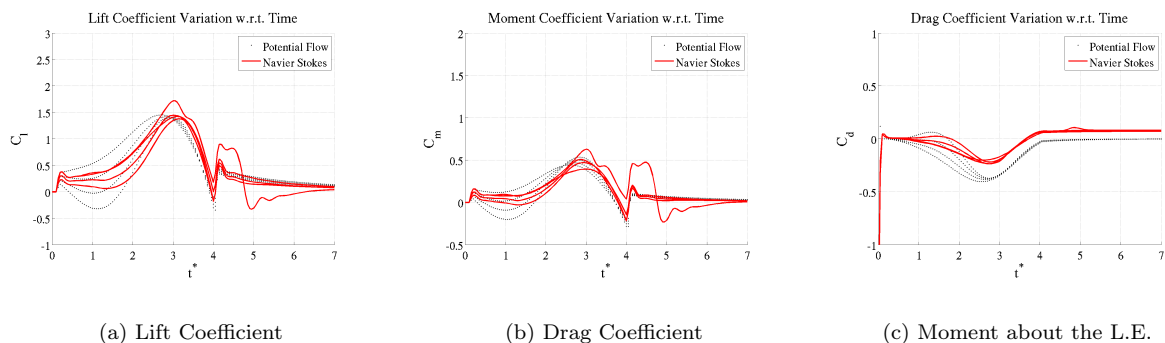


Figure 2. The force and moment coefficient evolution for the pitch-heave case. The results from the potential flow simulations are shown in black '.', while the results from the Navier-Stokes simulations are shown in red lines. In this series of plots, the force and moment histories for the less aggressive incidence angles (here the pitch angles are, $\theta = 9, 12, 15, 18$ degrees. Note that the pitch angle combined with the vertical velocity due to heaving causes a lower incidence angle.)

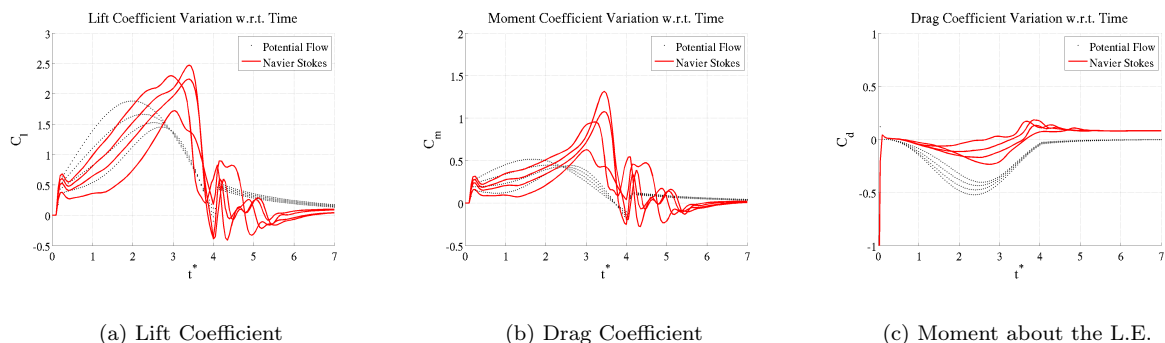


Figure 3. The force and moment coefficient evolution with respect to time for the pitch-heave case. The results from the potential flow simulations are shown in black '.', while the results from the Navier-Stokes simulations are shown in red lines. In this series of plots the force and moment histories for the more aggressive incidence angles are shown (here the pitch angles are $\theta = 0, 3, 6, 9$).

This example represents a simplified down-stroke motion of a flapping wing. The aim here is to isolate a single active down-stroke-like motion in order to study the effects of unsteadiness on the flow. The comparison of the different fidelity predictions of the force generation time history is shown in figures 2-3. The time history of force generation is shown in two separate plots, with the more aggressive incidence angles being plotted in figure 3. Additionally, several characteristic snapshots of the flows under consideration are shown in Figures 9-10.

| Parameter | Value |
|------------|-------------|
| θ_0 | 0, 3, ...18 |
| ω | 0.8 |
| h_0 | 0.5 |

Table 3. The parameter values for the harmonic heave and pitch example.

This example illustrates the flow physics for a simplified single down-stroke flapping motion. The isolated down-stroke illustrates the following:

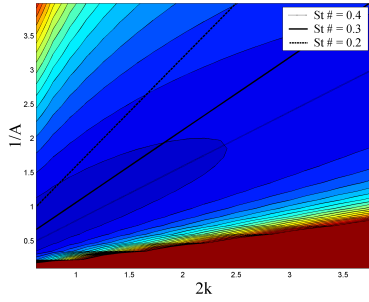
1. Similar to the previous unsteady pitch example, the potential flow appears to model the initial phases of the motion with good trend agreement. There is some deviation between the force predictions, which is likely due to viscous effects, but the trends remain unchanged.
2. In the more extreme incidence angle cases (figure 3), there is a pronounced deviation between the panel method prediction and the Navier-Stokes flow predictions in the region $t^* > 2.0$, which results from flow separation effects. In the Navier-Stokes simulations, the lift force is augmented by separation effects, while in the potential flow case, these effects are not observed.
3. When efficient force generation is desired, this example suggests that the pitch and heave should be selected such that the incidence angles are not too aggressive.

III.B. Example 2: Fluid Structure Interaction⁵

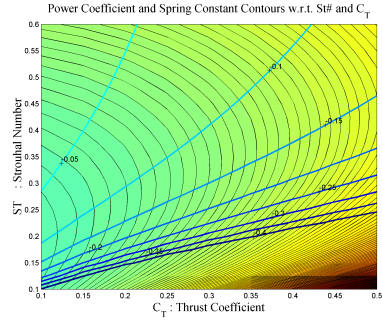
In the previous examples, a fully prescribed pitch and heave motion was examined. The examination showed that there was good trend based agreement between panel method analysis and the full flow analysis when the force generation was moderate to low. In the cases where incidences were aggressive and force generation was high, the panel method poorly represented the flow due to flow separation. The resulting flow could only be accurately predicted using higher fidelity methods. In the design of efficient flapping wings, the goal is to maintain attached flow throughout the flapping cycle to minimize the kinetic energy transfer into the fluid. In this example, we examine the generation of thrust using a prescribed heaving motion and a passive structural compliance to achieve appropriate pitch angles.

To design a feasible fluid structure interaction strategy, the collection of multi-fidelity methods is used. To begin, a wake only investigation of efficient thrust production was performed using the 2-Dimensional version of *HallOpt* (Figure 4 a). The results indicate that efficient thrust production is achieved when a particular range of Strouhal numbers is exploited (the optimal Strouhal Number range is quite similar to that observed in animals in nature⁴⁸). Furthermore, by observing the predicted optimal circulation distribution from the *HallOpt* solutions, it can be seen that a structural strategy which promotes a phase shift of approx $\pi/2$ radians between the pitching and heaving motions is desired. In order to passively achieve this phase lag, a leading edge torsional spring attaching the rigid foil to the heaving mechanism is considered. In figure 4 b., a preliminary investigation of the required spring stiffness is performed. The spring stiffness was approximated using a quasi-steady aerodynamics model and the optimal wake-circulation results from *HallOpt* (details can be found in⁵). Following the prediction of the leading edge spring constant, the resulting fluid structure interaction strategy was examined using the *FastAero* panel method (coupled with a simple drag polar viscous correction) and the 3DG Navier-Stokes method. The results of the efficiency prediction from each of the simulation tools are illustrated in Figure 4 c-d. The results illustrate that the simple design process which is used is sufficiently rich to predict the regime of maximum efficiency quite accurately, without using overly computationally expensive approaches. In Figures 4 e-f, the results of several sample simulations⁵ using both potential flow and Navier-Stokes methods are shown for this leading edge spring structural strategy. Since the spring is compliant, separation effects are avoided or minimized, by design, and as a result this thrust producing flapping foil strategy exhibits high efficiency.

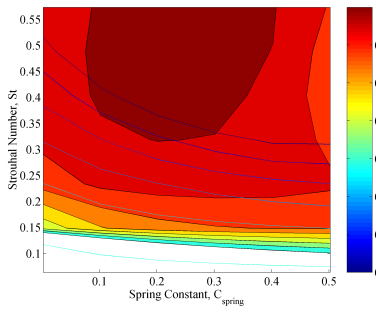
Several salient features of this simulation indicate that structural compliance may be a beneficial passive strategy in MAV flight:



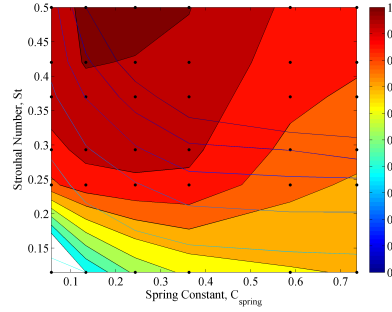
(a) HallOpt Design Space Sweep : $C_{T1} = 0.3$



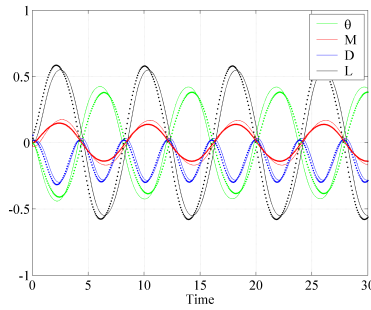
(b) Design Space Sweep to Determine Spring Stiffness



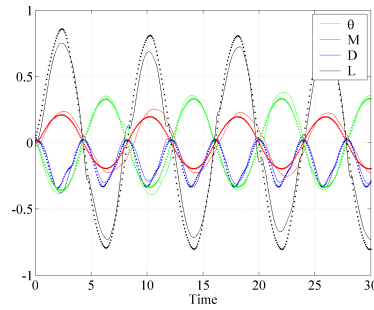
(c) FastAero2D Design Space Sweep Simulations, $\omega_r = 0.4$



(d) 3DG Design Space Sweep Simulations, $\omega_r = 0.4$



(e) Time Evolution of Forces for $C_{spring} = 0.363$, $St = 0.24$ and $\omega_r = 0.4$, FastAero2D vs. 3DG



(f) Time Evolution of Forces for $C_{spring} = 0.588$, $St = 0.24$ and $\omega_r = 0.4$, FastAero2D vs. 3DG

Figure 4. An illustration of the design process involved in generating thrust efficiently using a two dimensional airfoil with a leading edge torsional spring, undergoing prescribed heaving motions. In (a) a design space sweep examining the dependence of the power coefficient (color contours) on the flapping parameters of interest (heave, and frequency) is performed using *HallOpt*. In (b) the spring constant is approximated using a simple quasi-steady approximation of the aerodynamic force generation. Of particular interest in this plot is the prediction that a large range of thrust coefficients can be achieved using a single spring constant value and mildly changing the flapping parameters (in this plot the solid blue lines represent different spring constants, while the color contours represent the power required to generate that particular level of thrust). In (c-d) the efficiency (color contours) for different flapping motions are plotted as predicted by FastAero and 3DG respectively (note: Looking at similar regions on each plot illustrates a more decent match). The blue lines indicate lines of constant thrust coefficient (the important metric here is determining the most efficient strategy for a particular value of the thrust coefficient). In (e-f) the comparison of two of the many cases run in the efficiency plot are shown for comparing the FastAero potential flow results to the 3DG Navier-Stokes results. The computations show good agreement due to the flow being well behaved.)

1. Efficient flapping thrust production is possible by designing a compliant wing and changing the flapping parameters in order to generate different levels of thrust efficiently. In figure 4 c-d, it is seen that a single leading edge spring constant can be used to generate different levels of thrust efficiently by simply changing the flapping frequency or amplitude (by changing the Strouhal number).
2. The leading edge compliance which is incorporated into this example illustrates one possible strategy to minimize the adverse effects of large scale separation due to imprecise flapping kinematics. By adding a passive compliance, the airfoil can be effectively oscillated through a much larger range of parameters, providing more flexibility in the kinematics. In the previous example concerning prescribed kinematics, precise motions were required to achieve efficient flight force generation.
3. In nature, strategies which are similar in principle to the leading edge spring compliance are exploited. In bats, fish, and birds the compliant bones, vanes, and feathers (respectively) act as compliant beam members, effectively alleviating the force generation when flight and environmental conditions (flapping amplitudes, gusts, etc) are aggressive. This ability to handle unpredictable fluid environments effectively provides a compelling argument for developing a deeper understanding of compliance in flapping flight.

III.C. Example 3: Three-Dimensional Wing Design⁵

In the previous example an efficient thrust producing two-dimensional flapper was examined. In this example, a similar multi-fidelity design approach is followed; however, we consider three dimensional wings and limit the examination to the design of the aerodynamic shape⁵ (from a given optimal aerodynamic shape, it is possible to infer structural strategies which may be beneficial to explore). The process by which a design can be developed follows naturally from the previous 2-dimensional example. The design starts by determining the circulation distribution for an efficient wake using the HallOpt method. This design space exploration may consider diverse flapping parameters such as fore-aft flapping, multiple harmonics, etc.⁴ Following the exploration of the design space a particular efficient wake which produces the desired forces should be selected. Once the wake is selected, the optimal vorticity distribution is known. The remainder of the design problem is focused on determining the appropriate wing which generates the required vorticity distribution. One method which has been explored with some success⁵ is the generation of a reference, zero force producing geometry (a feathered geometry), and modifying the local angle of attack at various span wise wing sections to generate the desired forces and wake vorticity distribution. This process requires several iterative steps, but shows great promise in the development of efficient three dimensional wings.

Currently the successful shape design of a three-dimensional flapper has been performed; however, the outstanding problem of a passive structurally compliant, efficient force generating wing is still a work in progress. As in the previous example, the results of this investigation suggest a strategy which employs some amount of local leading edge compliance. It should be noted however, that, in this example the design strategy examined changes in local incidence only, and did not consider changes in section camber. By exploring both incidence and camber changes, a large array of possible structural strategies may be possible. Regardless of the structural strategy chosen, the resulting structural design will likely have a greater tolerance for inexact flapping kinematics while also providing natural stall alleviation capabilities.

III.D. Example 4: Bat Flight Based on Experimental Data⁶

Thus far, the computational framework has been applied to illustrate the *bottom-up* design philosophy. In this example, a potential flow solution of bat flight is presented to illustrate the *top-down* analysis approach. The details of the computations will be presented in more detail elsewhere.⁶ In this example a single flight of a single bat is examined.

III.D.1. Geometry Definition and Flow Simulation

The simulation of bat flight requires accurate geometric representations of the bat wing surfaces. In this work, the wing surface reconstructions are derived from experimental data of bats in flight in a wind tunnel.^{6, 23, 54} The bat flight kinematics are recorded using multiple high speed cameras. Pre-applied motion capture

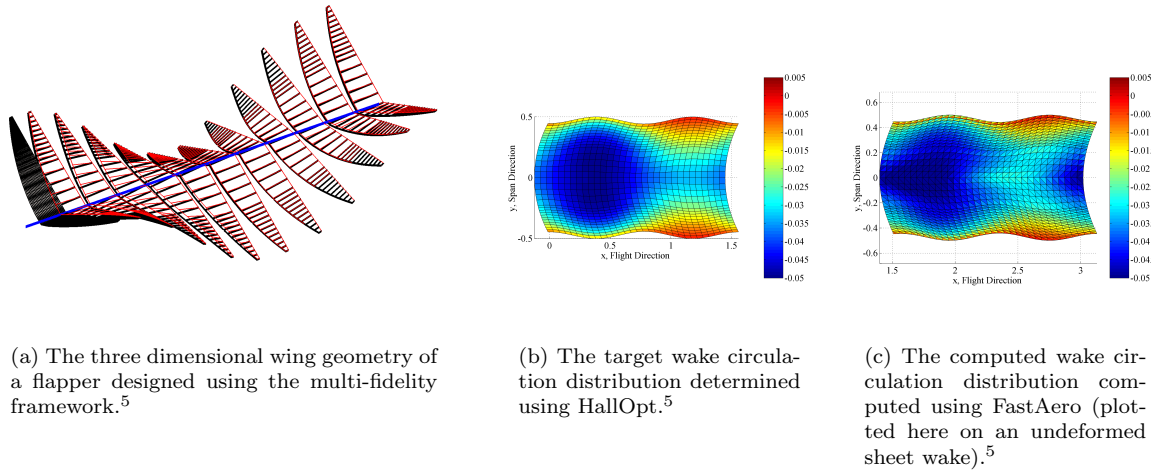
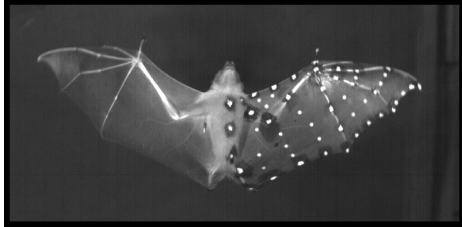


Figure 5. (a) The initial feathered wing (red) is illustrated in conjunction with the final loaded wing design (black). Snapshots are shown in a three-dimensional projection. This result suggests that an efficient strategy for producing flight forces would be to consider a leading edge compliance which has been tuned to present the appropriate local incidence.^{5,20} (b) The desired wake circulation distribution for the current configuration is computed using HallOpt. (c) The final wake circulation distribution (computed using FastAero) in the wake after the approximate inverse shape design is performed.⁵

markers are tracked in each of the camera views resulting in a set of three-dimensional marker paths. Using a quadratic patch approximation for different membrane surfaces, a computational model of the bat wing geometry is generated. Due to the lack of geometric data, the body of the bat is modeled as a simple extension of the wings. A detailed description of the procedure used for generating computational representations of the three dimensional wing surfaces is presented elsewhere.⁶ The result of the reconstruction of experimental data is a three dimensional membrane wing representation. A single snapshot of the three-dimensional computational representation is shown in Figure 6 b. The simulation of the flow is performed using the three dimensional panel method. An illustration of the potential flow solution is presented in Figure 6 c. The resulting force predictions are compared with an estimate of the forces derived from the center of mass accelerations⁶ and are shown in figure 6 d. In addition to the force predictions, the wing-beat cycle chart in figure 11 illustrates the unsteady pressure distribution on the wings over a chosen wing-beat cycle. The simulation of the flight of a bat illustrates the application of potential flow methods to a complex problem involving large deformations. The results also indicate several salient features of bat flight, namely:

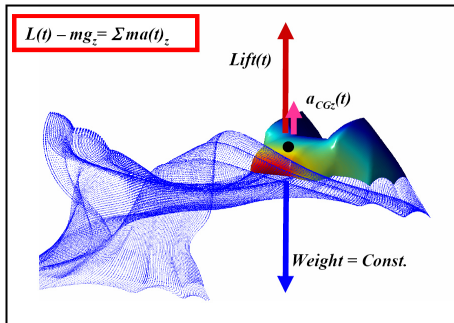
- The prediction of bat flight forces due to the potential flow model agrees with the prediction of forces using a center of mass acceleration prediction. This agreement does not confirm that the flow physics are correct; however, it does indicate that the force predictions are trend accurate. In order to determine the validity of the potential flow assumptions, experimental evidence of near wing flow features is being sought.
- The force generation results (Figure 6 d.), illustrate the time dependent, vertical force generation in bat flight. These predictions illustrate that the downstroke portion of the wingbeat cycle is heavily loaded, while the upstroke is virtually unloaded.
- The pressure distributions shown in figure 11 illustrate the nature of the bat flight force generation strategy. In this particular flight, the average forward velocity of the bat is relatively low. As such, the bat implements a strategy involving large forward-aft, sweeping motions in order to increase the relative velocity of the flow near the wingtips. The computed surface pressure distribution shows the effects of this strategy.
- The force generation in this bat flight example would be considered aggressive when compared with a fixed wing aircraft of similar size. As such, it is likely that some flow separation does exist. The extent to which this flow separation exists is yet unknown.



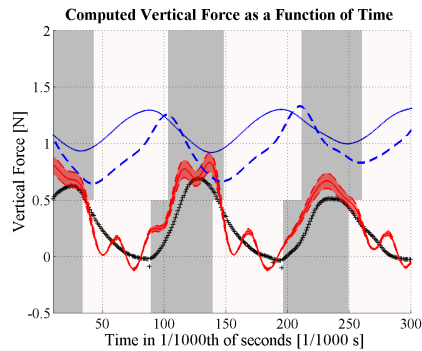
(a) A still frame image of a bat in flight taken from one view of the camera recording.



(b) An illustration showing the three-dimensional bat wing mesh which is developed using recorded kinematics of bat flight.



(c) An illustration showing a FastAero simulation of the bat in flight



(d) A comparison of the force generation prediction using a Panel Method and a center of mass acceleration approximation.

Figure 6. An overview of the simulation of bat flight aerodynamics using a panel method. In (a), a single snapshot of the experimental data is shown, illustrating the recording of motion capture markers. In (b), the resulting computational geometry representation which is constructed from the bat flight markers is shown. In (c), a single timestep of the FastAero simulation is shown, illustrating the definition of flight forces being examined. In (d) a comparison of the FastAero and center of mass acceleration force predictions is shown for this particular flight. The results are shown here for the vertical force as a function of time. The FastAero simulation results are depicted using black '.', while the acceleration of the center of mass is shown using red lines. The blue lines indicate the traces of the wingtip (dashed line) and wing wrist (solid line) as a function of time. As can be seen there is a good qualitative and quantitative agreement between the different force prediction approaches. In the case of bat flight, it is unclear whether flow separation is a dominant feature of the flight strategy; however, the potential flow does illustrate good predictive capability despite the possibility that some of the actual flow physics is not accurately captured.

IV. Conclusions

In this paper, an overview of a collection of computational tools for analysing flapping flight has been presented. The use of rapid, lower fidelity computational methods in flapping flight design and analysis is being explored in order to determine the applicability of such tools to minimizing the computational cost of performance predictions. Since efficient flapping flight aerodynamics encourages the minimization of induced and viscous power losses, methods such as potential flow approaches may be able to provide initial insight into the design space. The examples shown illustrate it is possible to design efficient flapping wing concepts using lower fidelity methods as a starting point in the design investigation; however, the use of these methods should be followed by confirmations using higher fidelity Navier-Stokes approaches.

V. Acknowledgments

The authors of this paper would like to recognize and thank the members of the AFOSR-MURI effort on flapping flight for their inputs and discussions of flapping flight and bat flight. In addition, we would also like to thank Dr. Michael Ol for organizing the session. Furthermore, we would like to thank the Singapore-MIT Alliance, the NSF, NSERC and the AFOSR for their support of different aspects of this work.

References

- ¹HALL, K. C., AND HALL, S. R., *Minimum induced power requirements for flapping flight* Journal of Fluid Mechanics, 1996, Vol. 323, pp. 285-315.
- ²HALL, K. C., PIGOTT, S. A., AND HALL, S. R., *Power Requirements for Large-Amplitude Flapping Flight* Journal of Aircraft, Vol. 35, No. 3, 1998, pp. 352-361.
- ³HALL, K. C., AND PIGOTT, S. A., *Power Requirements for Large-Amplitude Flapping Flight*, AIAA Paper 97-0827, Presented at the 35th Aerospace Sciences Meeting and Exhibit, Reno, NV, Jan. 6-9, 1997.
- ⁴D.J. WILLIS, J.PERAIRE, M.DRELA, AND J.K.WHITE, *A numerical Exploration of Parameter Dependence in Power Optimal Flapping Flight*, AIAA-2006-2994, San Francisco, 2006.
- ⁵D.J.WILLIS, E.R.ISRAELI, M.DRELA, J.PERAIRE, S.M.SWARTZ, K.S.BREUER, *A computational Framework for Fluid Structure Interaction in Biologically-Inspired Flapping Flight*, presented at AIAA Conference, AIAA-2007-3803, Miami, FL, June 2007.
- ⁶D.J.WILLIS, D.K.RISKIN, K.S.BREUER, S.M.SWARTZ, AND J.PERAIRE *A Computational Study of the Aeromechanics of a Bat: Cynopterus brachyotis at Different Flight Speeds*, In preparation.
- ⁷D.J.WILLIS, J.PERAIRE AND J.K.WHITE, *A Combined pFFT-multipole tree code, unsteady panel method with vortex particle wakes*, AIAA Paper 2005-0854, Reno, NV, Jan. 2005.
- ⁸D.J.WILLIS, J.PERAIRE, AND J.K.WHITE, *A quadratic basis function, quadratic geometry, high order panel method*, presented at 44th AIAA Aerospace Sciences Meeting, AIAA-2006-1253, Reno, Nevada, 2006.
- ⁹SWARTZ, S.M., IRIARTE-DIAZ, J., RISKIN, D.K., SONG, A., TIAN, X., WILLIS, D.J., AND BREUER, K.S., *Wing Structure and the Aerodynamic Basis of Flight in Bats*, 46th AIAA Aerospace Sciences Meeting and Exhibit, Reno, NV, 2007.
- ¹⁰J.PERAIRE, J.PIERO, L.FORMAGGIA, K.MORGAN, AND O.C.ZIENKIEWICZ, *Finite Element Euler Computations in Three Dimensions*, Int. J. Num. Meth. in Engr. 26, 2135-2159, 1988.
- ¹¹A. JAMESON, *Computational Aerodynamics for Aircraft Design*, Science, Vol 245 no. 4916, pp. 361-371, 1989.
- ¹²J. KATZ AND A. PLOTKIN, *Low Speed Aerodynamics*, Cambridge University Press, Cambridge, 2001.
- ¹³J.N. NEWMAN, *Distribution of sources and Normal Dipoles Over a Quadrilateral Panel*, J. Eng. Math., 20, 1985.
- ¹⁴J.L. HESS, *The problem of three dimensional flow and its solution by means of surface singularity distribution* Comput. Meth. Appl. Mech. Eng., 4: 283-319, 1974.
- ¹⁵L. MORINO AND C.C.LUO, *Subsonic potential aerodynamics for complex configurations. A general theory*. AIAA J. 12:191-197.
- ¹⁶D.J.WILLIS, J.PERAIRE AND K.S.BREUER, *A computational investigation of bio-inspired formation flight and ground effect*, presented at AIAA Conference, AIAA-2007-4182, Miami, FL, June 2007.
- ¹⁷D.J.WILLIS, J.PERAIRE AND J.K.WHITE, *A Combined pFFT-multipole tree code, unsteady panel method with vortex particle wakes*, Int. J. Numer. Meth. Fluids, 53, 1399-1422, 2007.
- ¹⁸D.J.WILLIS, J.PERAIRE AND J.K.WHITE, *A Combined pFFT-multipole tree code, unsteady panel method with vortex particle wakes*, AIAA Paper 2005-0854, Reno, NV, Jan. 2005.
- ¹⁹VEST M., AND KATZ J., *Aerodynamics of a Flapping-Wing Micro UAV*, AIAA 99-0994, presented at the AIAA 37th Aerospace Sciences Meeting in Reno, NV, Jan. 1999.
- ²⁰DELAURIER, J.D., *An Aerodynamic Model for Flapping-Wing Flight* Aeronautical Journal, 1993, pp.125-130
- ²¹I.H. TUNCER AND M.F. PLATZER, *Thrust Generation due to Airfoil Flapping*, AIAA Journal, Vol. 34, No. 2, February 1996, pp. 324-331.
- ²²TUNCER, I.H., KAYA, M. *Optimization of Flapping Airfoils for Maximum Thrust and Propulsive Efficiency*, AIAA Journal, Vol. 43, No. 11, Nov. 2005.

- ²³DANIEL K. RISKIN, DAVID J. WILLIS, JOSE IRIARTE-DIAZ, TYSON L. HEDRICK, MYKHAYLO KOSTANDOV, JIAN CHEN, DAVID H. LAIDLAW, KENNETH S. BREUER, AND SHARON M. SWARTZ, *Describing bat wing kinematics accurately: Quantifying complexity with Proper Orthogonal Decomposition*, Submitted.
- ²⁴D.J.WILLIS, *An Unsteady, Accelerated, High Order Panel Method with Vortex Particle Wakes*, MIT PhD. Thesis, 2006.
- ²⁵WINTER, Y., *Energetic cost of hovering flight in a nectar-feeding bat measured with fast-response respirometry*, Journal of Comparative Physiology B-Biochemical Systemic and Environmental Physiology, 1998. 168(6): p. 434-444.
- ²⁶WINTER, Y. AND O. VON HELVERSEN, *The energy cost of flight: do small bats fly more cheaply than birds?*, Journal of Comparative Physiology B-Biochemical Systemic and Environmental Physiology, 1998. 168(2): p. 105-111.
- ²⁷VOIGT, C.C. AND Y. WINTER, *Energetic cost of hovering flight in nectar-feeding bats (Phyllostomidae : Glossophaginae) and its scaling in moths, birds and bats*. Journal of Comparative Physiology B-Biochemical Systemic and Environmental Physiology, 1999. 169(1): p. 38-48.
- ²⁸U.M.NORBERG, *Vertebrate Flight*, Springer-Verlag, Berlin, 1990.
- ²⁹J TOOMEY AND J. D. ELDREDGE, *Numerical and Experimental Investigation of the role of flexibility in flapping wing flight*, AIAA 2006-3211, 36th AIAA Fluid Dynamics Conference and Exhibit, San Francisco, 2006.
- ³⁰K.D. JONES, T.C. LUND AND M.F. PLATZER, *Fixed and Flapping Wing Aerodynamics for Micro Air Vehicle Applications*, AIAA Progress in Astronautics and Aeronautics, Vol. 195, Ed. T. Mueller, 2001, pp. 307-339.
- ³¹M. ABDULRAHIM, K. BOOTHE, R. LIND AND P. IFJU, *Flight Characterization of Micro Air Vehicles using Morphing for Agility and Maneuvering*, SAE World Aviation Congress, Reno, NV, SAE-2004-01-3138, November 2004.
- ³²D. VIHIERU, J. TANG AND Y. LIAN H. LIU W. SHYY, *Flapping and Flexible Wing Aerodynamics of Low Reynolds Number Flight Vehicles*, AIAA-2006-503, 44th AIAA Aerospace Sciences Meeting and Exhibit, Reno, Nevada, Jan. 9-12, 2006
- ³³M. ABDULRAHIM AND R. LIND, *Flight Testing and Response Characteristics of a Variable Gull-Wing Morphing Aircraft*, AIAA Guidance, Navigation and Control Conference, Providence, RI, AIAA-2004-5113, August 2004.
- ³⁴H. ASHLEY, M. LANDAHL, *Aerodynamics of wings and bodies*, Dover Publications, New York, 1985.
- ³⁵W. P. RODDEN, *The Development of the Doublet-Lattice Method*, International Forum on Aeroelasticity and Structural Dynamics, June 1997.
- ³⁶C.A.BREBBIA, *Boundary Element Techniques: Theory and Applications in Engineering*, Springer, 1984.
- ³⁷A. LEONARD, *Computing three-dimensional incompressible flows with vortex elements*, Ann. Rev. Fluid Mech., 17: 523-559, 1985.
- ³⁸A. GHARAKHANI, A.F. GHONIEM, *Three-dimensional vortex simulation of time dependent incompressible internal viscous flows*, J. Comp. Phys., 134: 75-95. 1997.
- ³⁹C. REHBACH, *Calcul Numerique d'ecoulement tridimensionnels instationnaires avec nappes tourbillionnaires* La Recherche Aerospatiale, pp, 289-298, 1977.
- ⁴⁰J.R. PHILIPS AND J.K.WHITE, *A precorrected-FFT Method for Electrostatic Analysis of Complicated 3D structures*, IEEE Transactions on Computer Aided Design of Integrated Curcuits and Systems, IEEE, Vol. 16, 1997.
- ⁴¹J. BARNES AND P. HUT, *A hierarchical $O(N \log N)$ force-calculation algorithm*. Nature, 324(4), December 1986.
- ⁴²L. GREGGARD AND V. ROHKLIN, *A Fast Algorithm for particle simulations*, J. comp. Phys., 73: pp 325-384, 1987.
- ⁴³Y. SAAD, AND M. SCHULTZ, *GMRES: A generalized Minimal Residual Algorithm for Solving Non-Symmetric Linear Systems*, SIAM, J. Sci. Comp., Vol 7, 1986.
- ⁴⁴R. MITTAL AND G. IACCARINO, *Immersed Boundary Methods*, An. Rev. of Fluid Mechanics, 37:239-261, Jan. 2005.
- ⁴⁵M.-C. LAI AND C.S. PESKIN, *An immersed boundary method with formal second order accuracy and reduced numerical viscosity*, J. comput. Phys., 160:705-719, 2000.
- ⁴⁶D.J.WILLIS, P.-O.PERSSON, *Investigations of 2-Dimensional Airfoils Under Prescribed Motion*, in preparation.
- ⁴⁷HOVER FS, HAUGSDAL O, TRIANTAFYLLOU MS, *Effect of angle of attack profiles in flapping foil propulsion* J Fluid Struct, 19 (1): 37-47, Jan. 2004
- ⁴⁸GRAHAM K. TAYLOR ROBERT L. NUDDS AND ADRIAN L. R. THOMAS, *Flying and swimming animals cruise at a Strouhal number tuned for high power efficiency*, Nature 425, 707-711, 2003.
- ⁴⁹B. COCKBURN AND C.-W. SHU, *Runge-Kutta discontinuous Galerkin methods for convection-dominated problems*, J. Sci. Comput., 16 (2001), pp. 173-261.
- ⁵⁰J. PERAIRE AND P.-O. PERSSON, *The compact discontinuous Galerkin (CDG) method for elliptic problems*, SIAM J. Sci. Comput., (2008), to appear.
- ⁵¹P.-O. PERSSON AND J. PERAIRE, *Newton-GMRES preconditioning for discontinuous Galerkin discretizations of the Navier-Stokes equations*, SIAM J. Sci. Comput., (2008), to appear.
- ⁵²P.-O. PERSSON, J. PERAIRE, AND J. BONET, *Discontinuous Galerkin solution of the Navier-Stokes equations on deformable domains*, in 45th AIAA Aerospace Sciences Meeting and Exhibit, Reno, Nevada, 2007. AIAA-2007-513.
- ⁵³P.-O. PERSSON, J. PERAIRE, AND J. BONET, *A High Order Discontinuous Galerkin Method for Fluid-Structure Interaction*, in 18th AIAA Computational Fluid Dynamics Conference, Miami, Florida, 2007. AIAA-2007-4327.
- ⁵⁴Tian, X., Iriate-Diaz, J., Middleton, J., Galvao, R., Israeli, E., Roemer, A., Sullivan, A., Song, A., and Breuer, K.S., "Direct measurements of the kinematics and dynamics of bat flight," bioinsp. Biomim, 1 S10-S18, 2006.
- ⁵⁵P.B.S. LISSAMAN, *Low-Reynolds-Number Airfoils*, Ann. Rev. Fluid Mech., 15:223-39, 1983.
- ⁵⁶J. KATZ AND S. YON, *Impulsive Start of a Symmetric Airfoil at High Angle of Attack*, AIAA Journal, Vol 34., No. 2, February 1996.

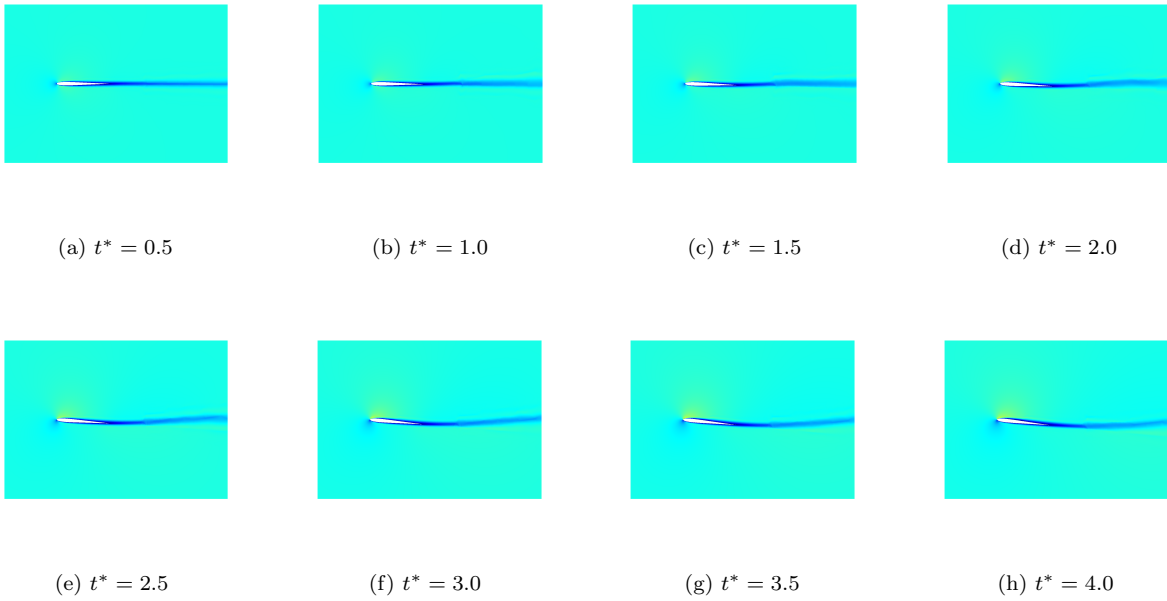


Figure 7. Snapshots of the time evolution of the pitch kinematics and the resulting flow structures for $\theta_0 = 3^\circ$ (pitch angle change of 6 degrees) predicted using the Navier-Stokes Solver. The flow is well behaved and remains attached throughout the unsteady pitching motion; however, as can be seen from the force coefficient history, the flow eventually separates and becomes unsteady suggesting that the unsteady pitch motions and associated wake structures assist with keeping the flow attached.

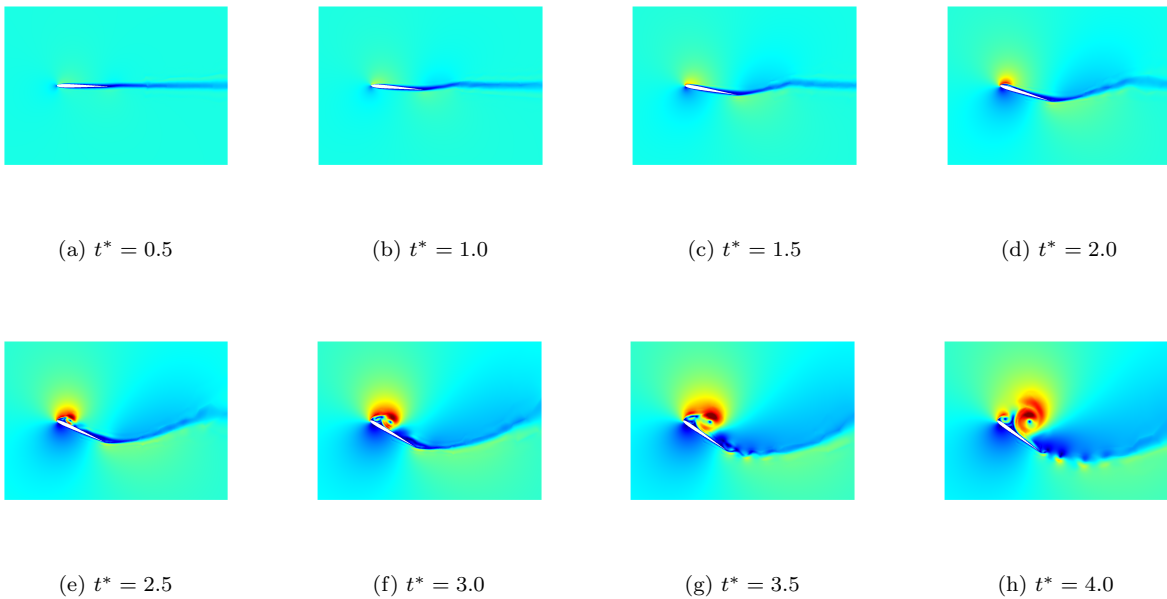


Figure 8. Snapshots of the time evolution of the pitching kinematics and the associated flow for a more aggressive pitch angle of $\theta_0 = 18^\circ$ (pitch angle change of 36 degrees). It is clear in this example that the flow starts to separate, forming a leading edge separation “bubble” region ($t^* \simeq 2.0 - 2.5$) prior to developing into fully separated flow ($t^* \geq 3.0$). The plots combined with the force coefficient history plots illustrate that potential flow approximations fail in this case once large regions of separation form. In conjunction with significant separation in this case is a rapid rise in drag coefficient. This is expected due to the significant separation involved.

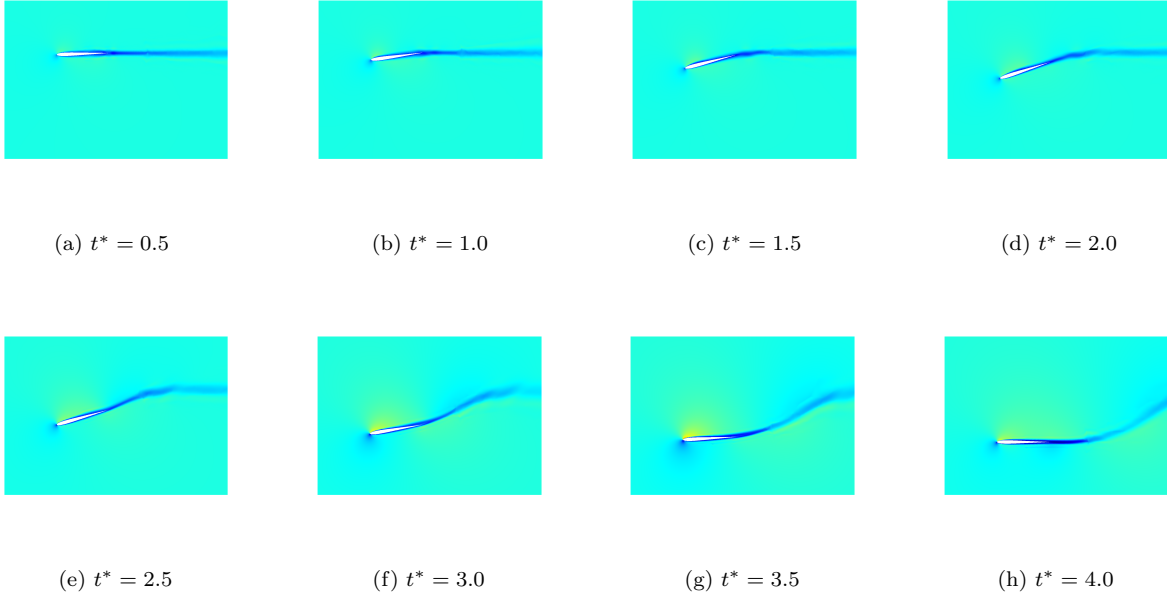


Figure 9. The time evolution of the flow for the single pitch-heave combination case. Due to the favorable incidence of the airfoil throughout the approximate dowstroke, the flow remains attached. This case corresponds to the $\theta_0 = 18^\circ$.

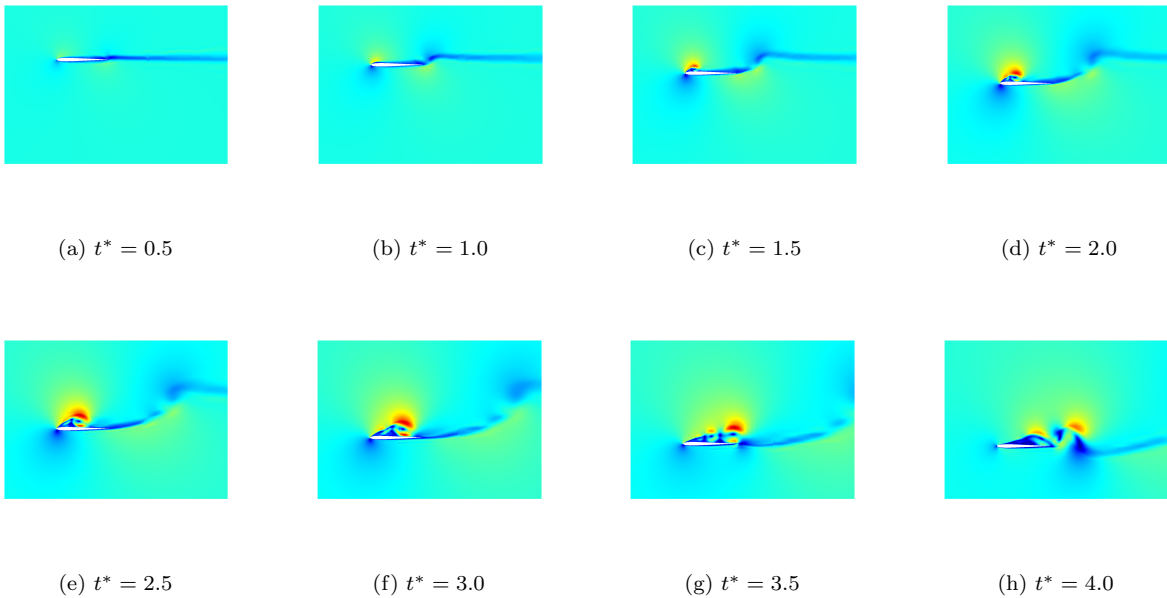


Figure 10. A series of snapshots of the case where an aggressive incidence is set during the pitch-heave downstroke case ($\theta_0 = 0^\circ$). In this example, flow separation at the leading edge starts to develop soon after the initiation of the motion ($t^* \simeq 1.5$), and develops into massively separated flow by the end of the simulation.

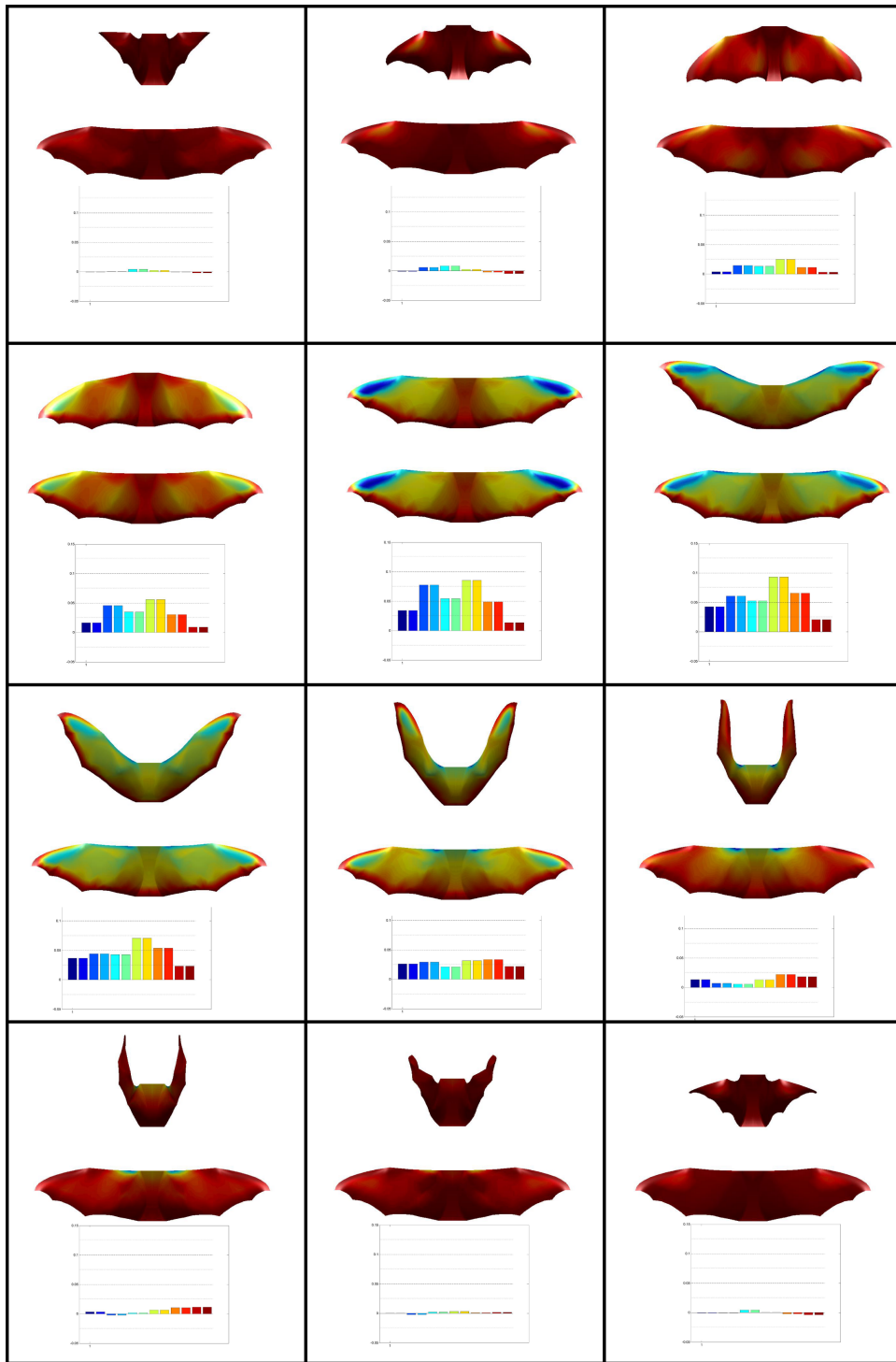


Figure 11. An illustration of the pressure distribution on the bat wings during a single wingbeat cycle.⁶ The upper-most image of each snapshot is the top-down view of the wing in the current configuration, the middle image is the pressure distribution plotted on a reference configuration (to show the pressure distribution more clearly), and the lower image in each box shows the regional force generation on the wings with the first two bars showing the leading edge membrane contribution and subsequent pairs of bars showing the contributions of the membrane regions from the outer region of the wing to the inner regions of the wing.⁶ The pressure distribution is shown with a large pressure jump from the lower to upper wing surface indicated by blue, and a zero pressure jump indicated in red. This illustration shows the significant forward aft motion of the wings during the wingbeat cycle. This forward-aft motion of the wings is accompanied by a corresponding increased loading in the outboard region of the wings. In addition the results indicate a nearly complete alleviation of forces during the upstroke. The image also illustrates the outboard loading on this particular bat flight (which is likely due to the increased dynamic pressure on the outboard portion of the wings). This simulation result illustrates the possibility for separation near the trailing edge on the outboard portions of the wing, where sharp adverse pressure gradients exist.